Synthesis and Redox Properties of (3-Phenothiazinomesityl)- and (4-Phenothiazinoduryl)dimesitylphosphines and the Corresponding Arsines

Shigeru Sasaki, Fumiki Murakami, and Masaaki Yoshifuji*

Department of Chemistry, Graduate School of Science, Tohoku University, Aoba, Sendai 980-8578, Japan

sasaki@mail.tains.tohoku.ac.jp

Experimental Section

General

^{1}H and ^{13}C NMR spectra were measured at 200 or 600 MHz and at 50 or 150 MHz, respectively. ^{31}P NMR spectra were measured at 81 MHz. ^{1}H and ^{13}C NMR chemical shifts are expressed as δ downfield from external tetramethylsilane and calibrated with residual proton of the deuterated solvents and deuterated carbon, respectively. ^{31}P NMR chemical shifts are expressed as δ downfield from 85% H_3PO_4. Low-resolution mass spectra were measured with electron impact (EI) ionization at 70 eV or with fast atom bombardment (FAB) ionization using *m*-nitrobenzyl alcohol matrix. High-resolution mass spectra were measured with electron impact (EI) ionization at 70 eV. Melting points were measured by micro melting point apparatus and were not corrected. Microanalyses were performed at the Instrumental Analysis Center of Chemistry, Graduate School of Science, Tohoku University. Flush column chromatography was carried out using compressed air over silica gel (Fuji Silysia, BW-300) unless specified otherwise. Tetrahydrofuran and diethyl ether were distilled from sodium diphenylketyl under argon just prior to use. 1,3-Dibromomesitylene was purchased from Aldrich. 1,4-Dibromodurene[1] was prepared by bromination of durene with bromine in the presence of iron powder in chloroform. 1,3-Dibromomesitylene was purchased from Aldrich. Arsenic trichloride and phosphorus trichloride were purchased from Wako Pure Chemical Industries and used without further purification. Cyclic voltammograms were measured with glassy carbon and Pt wire as a working and a counter electrode, respectively. As a reference electrode, Ag / 0.01 M $AgNO_3$ / 0.10 M *n*-Bu_4NClO_4 CH_3CN were used, where ferrocene / ferricinium redox couple appeared at 0.18 V. The solution of the substrate (ca. 10^{-3} $molL^{-1}$) dissolved in dichloromethane with 0.10 M *n*-Bu_4NClO_4 as a supporting electrolyte was degassed by bubbling with nitrogen and measured under nitrogen at room temperature or at 195 K with Dry Ice/ acetone Dewar. X-band EPR samples were degassed by three times of freeze and thaw cycles after transferring the solvent by bulb-to-bulb distillation, and oxidized in the sample tubes.

Cyclic voltammograms

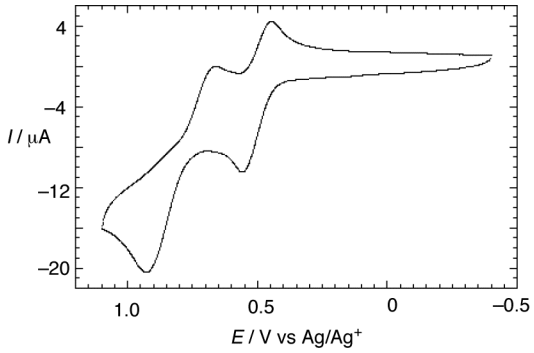

Figure 1. Cyclic voltammogram of bis(4-*t*-butylphenyl)[3-(dimesitylarsino)mesityl]amine (**3aA**) at 195 K.

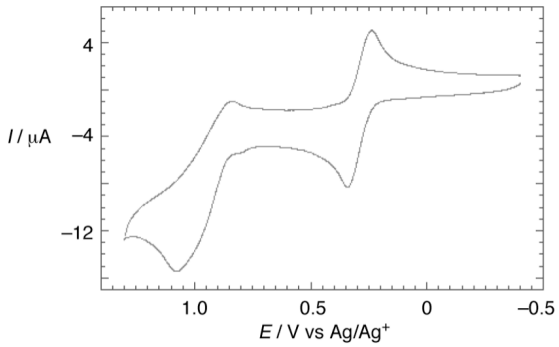

Figure 2. Cyclic voltammogram of bis(4-methoxyphenyl)[3-(dimesitylarsino)mesityl]amine (**3cA**) at 195 K.

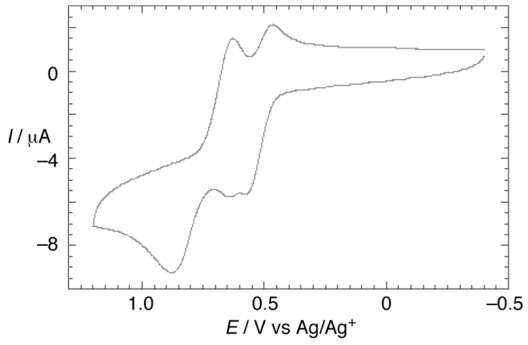

Figure 3. Cyclic voltammogram of bis(4-*t*-butylphenyl)[4-(dimesitylarsino)-2,3,5,6-tetramethylphenyl]amine (**4aA**) at 195 K.

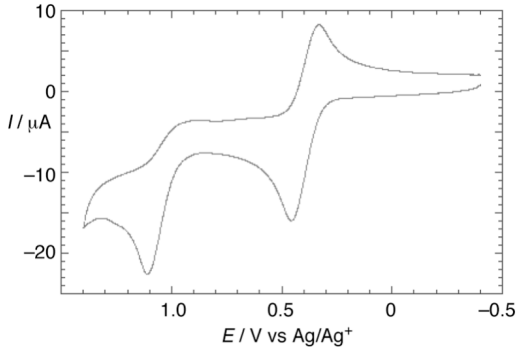

Figure 4. Cyclic voltammogram of mesitylphenothiazine at 293 K.

EPR spectra

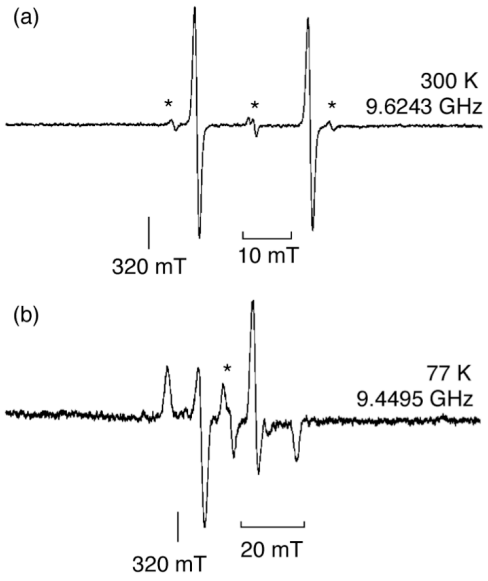

Figure 5. EPR spectra obtained by oxidation of trimesitylphosphine (**1**) with tris(4-bromophenyl)aminium perchlorate in dichloromethane (a) at 300 K (g = 2.0107 and $a(^{31}P)$ = 23.4 mT) and (**b**) 77 K ($g_{\perp}$ = 2.0094, $g_{//}$ = 2.0030, and $a_{\perp}(^{31}P)$ = 17.4, $a_{//}(^{31}P)$ = 40.8 mT). * Impurity.

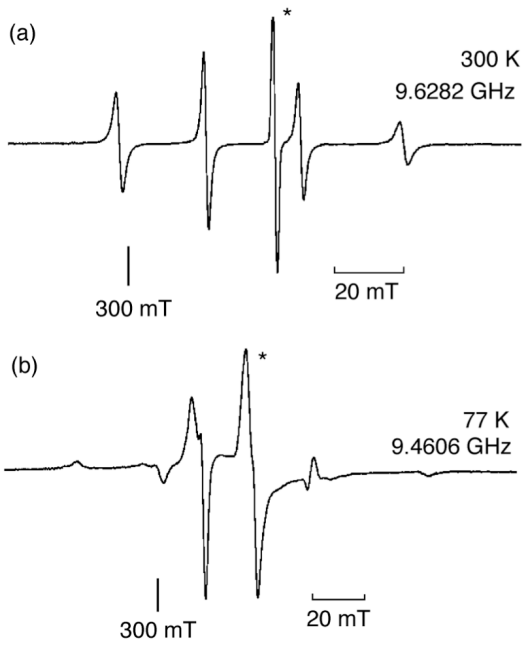

Figure 6. EPR spectra obtained by oxidation of trimesitylarsine (**2**) with tris(4-bromophenyl)aminium perchlorate in dichloromethane (a) at 300 K (g = 2.0378, $a(^{75}\text{As})$ = 27.5 mT) and (b) 77 K ($g_{\perp}$ = 2.056, $g_{//}$ = 2.004, $a_{\perp}(^{75}\text{As})$ = 18.7, $a_{//}(^{75}\text{As})$ = 45.6 mT). * Impurity.

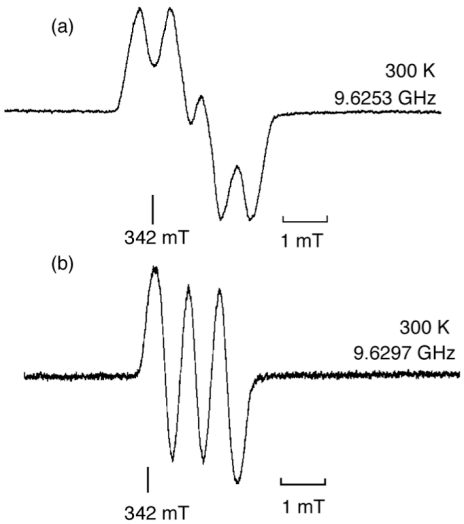

Figure 7. EPR spectra obtained by oxidation of (a) **3bP** (g = 2.0052, $a(^{14}\text{N})$ = 0.75 mT, $a(^{31}\text{P})$ = 0.75 mT) and (b) **3bA** (g = 2.0054, $a(^{14}\text{N})$ = 0.74 mT) with silver(I) perchlorate in dichloromethane at 300 K.

[1]H NMR spectra

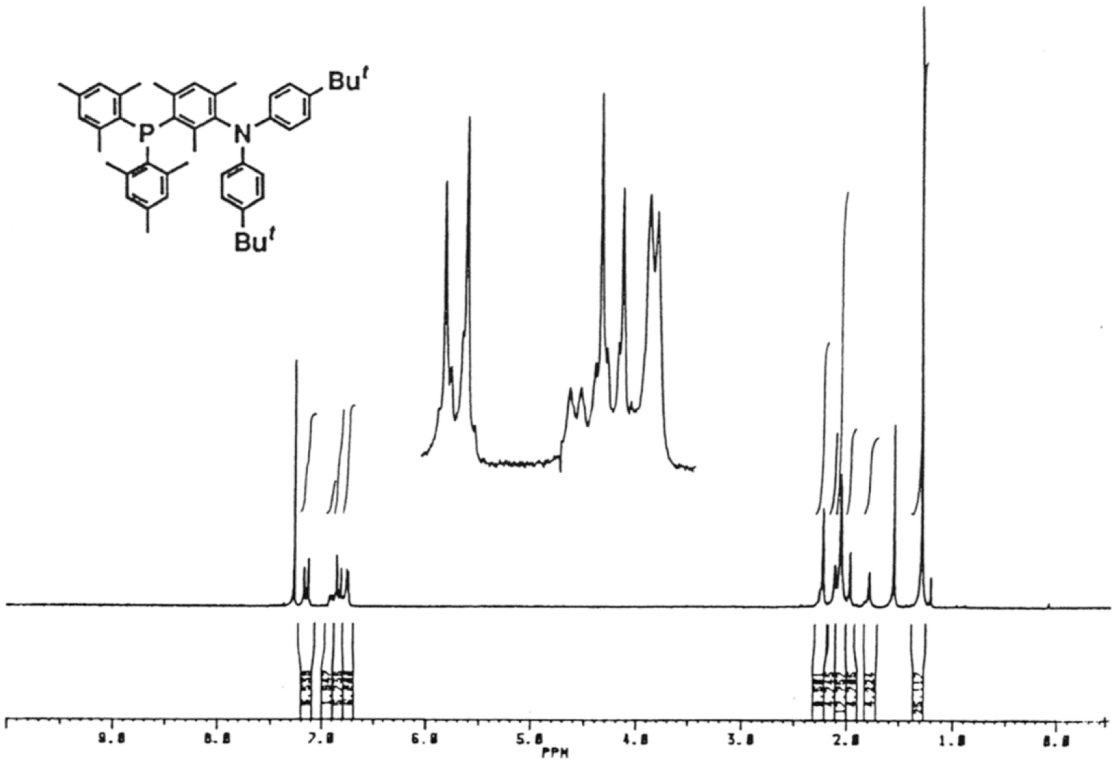

Figure 8. ^{1}H NMR (200 MHz, $CDCl_3$) spectrum of **3aP**.

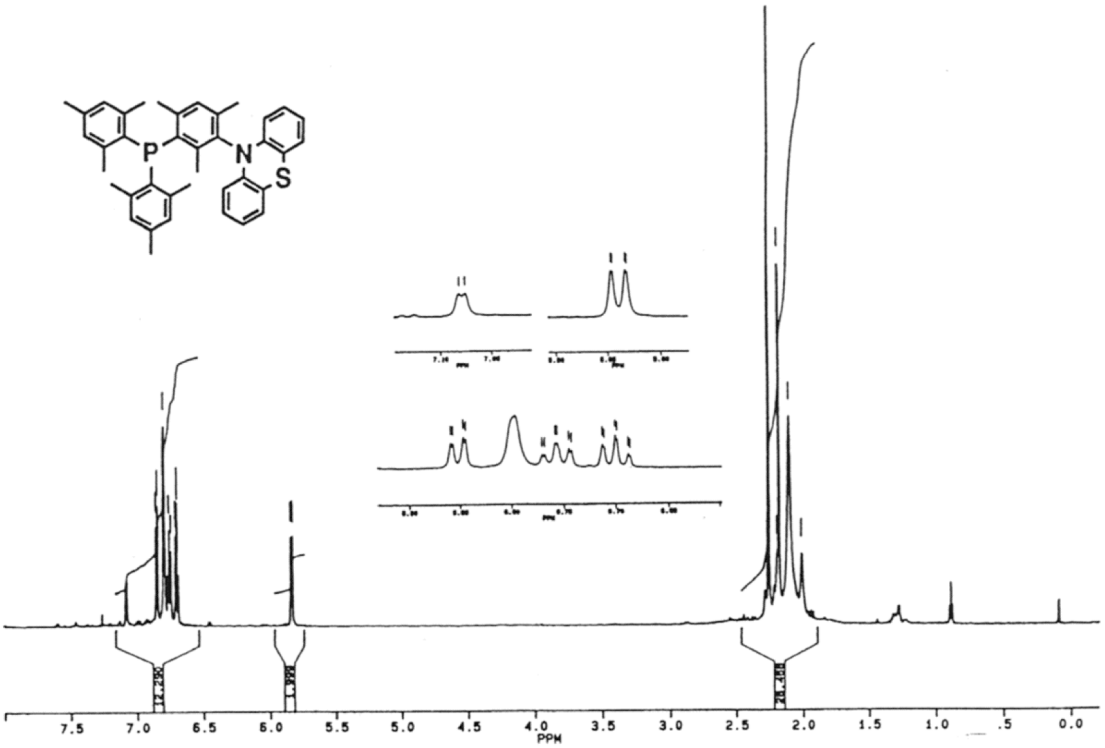

Figure 9. ^{1}H NMR (600 MHz, $CDCl_3$) spectrum of **3bP**.

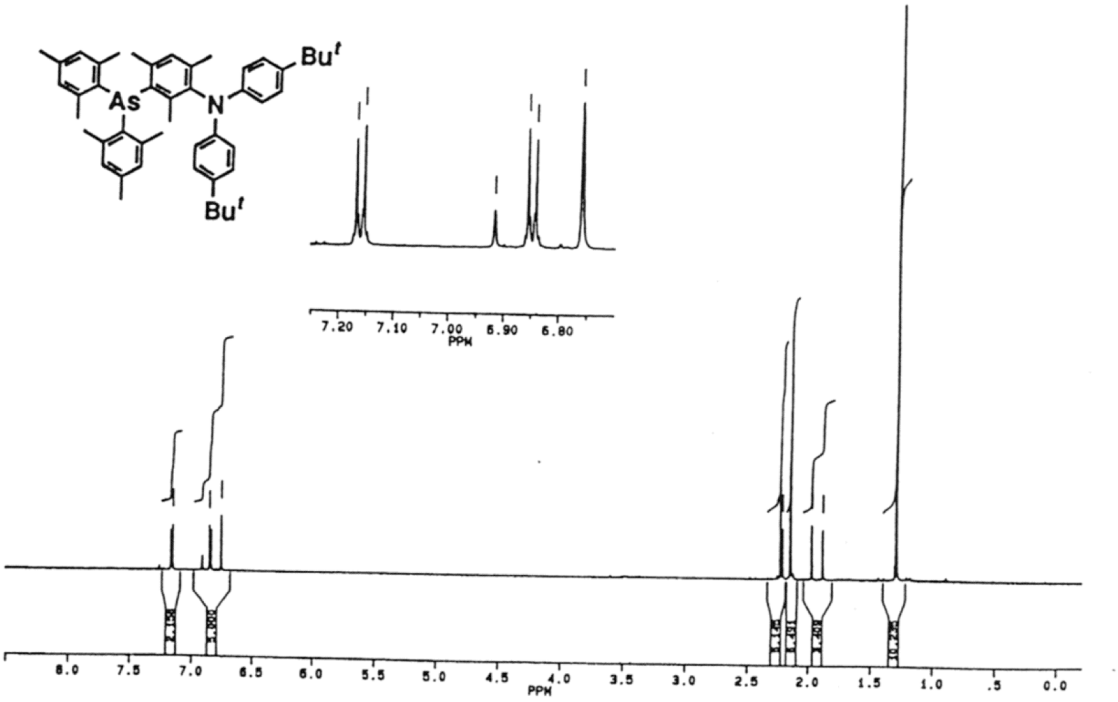

Figure 10. ^{1}H NMR (600 MHz, $CDCl_3$) spectrum of **3aA**.

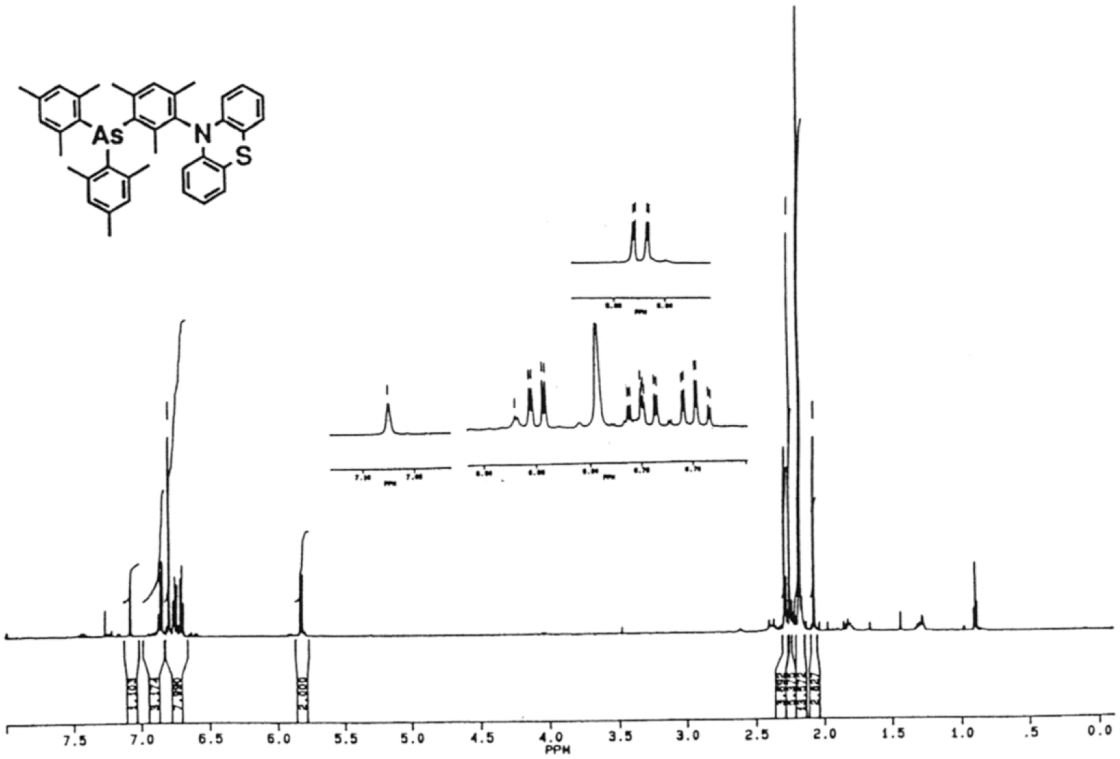

Figure 11. ^{1}H NMR (600 MHz, $CDCl_3$) spectrum of **3bA**.

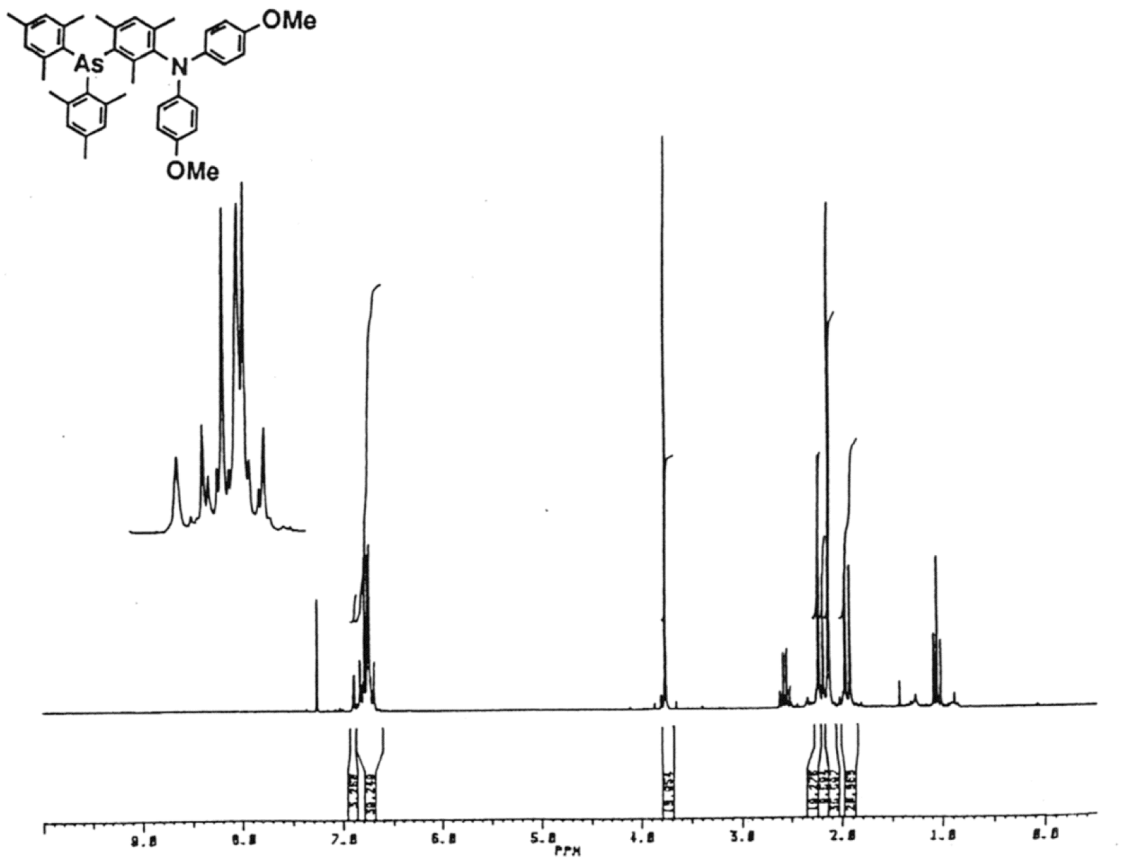

Figure 12. ^{1}H NMR (200 MHz, $CDCl_3$) spectrum of **3cA**.

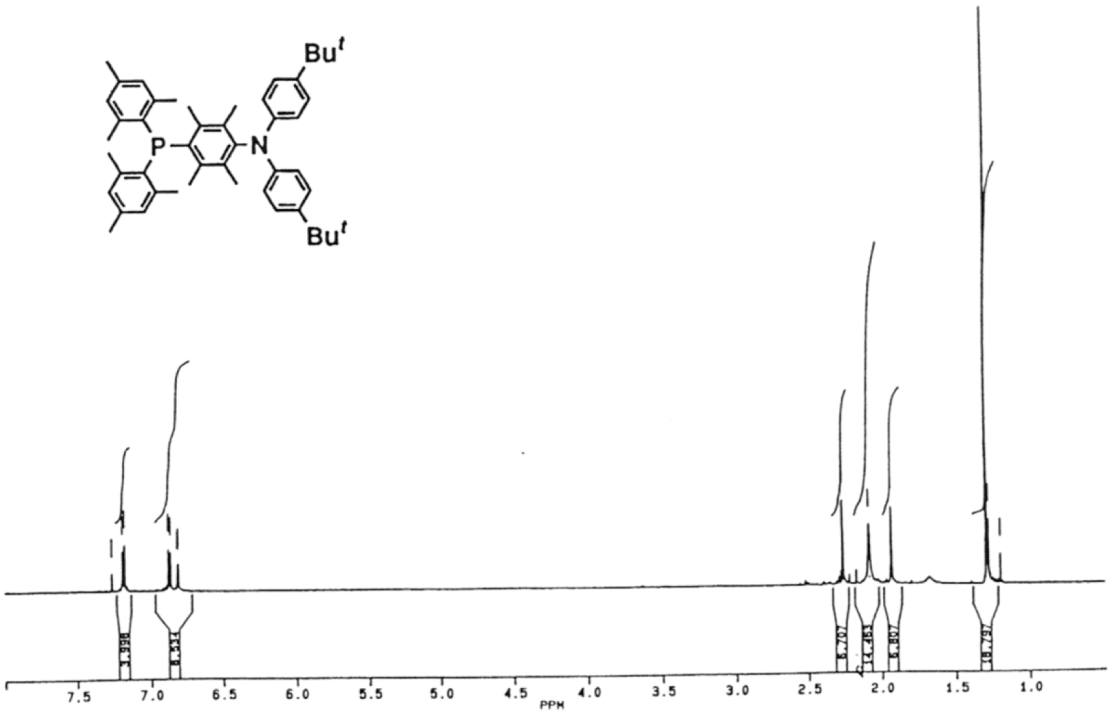

Figure 13. ^{1}H NMR (600 MHz, $CDCl_3$) spectrum of **4aP**.

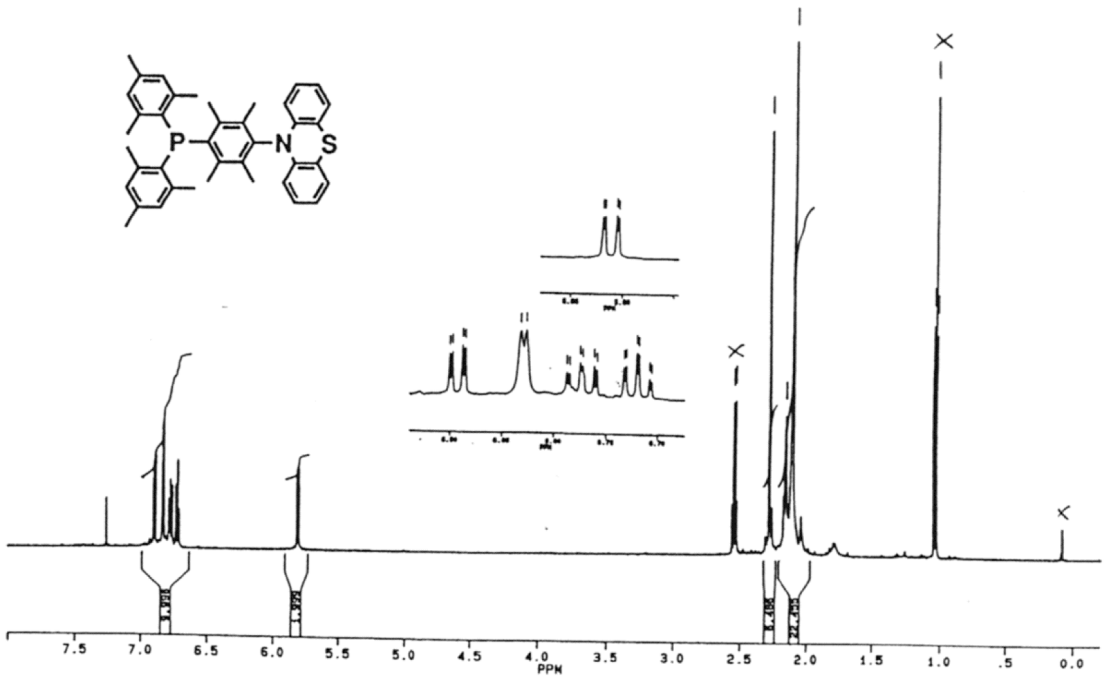

Figure 14. ^{1}H NMR (600 MHz, $CDCl_3$) spectrum of **4bP**.

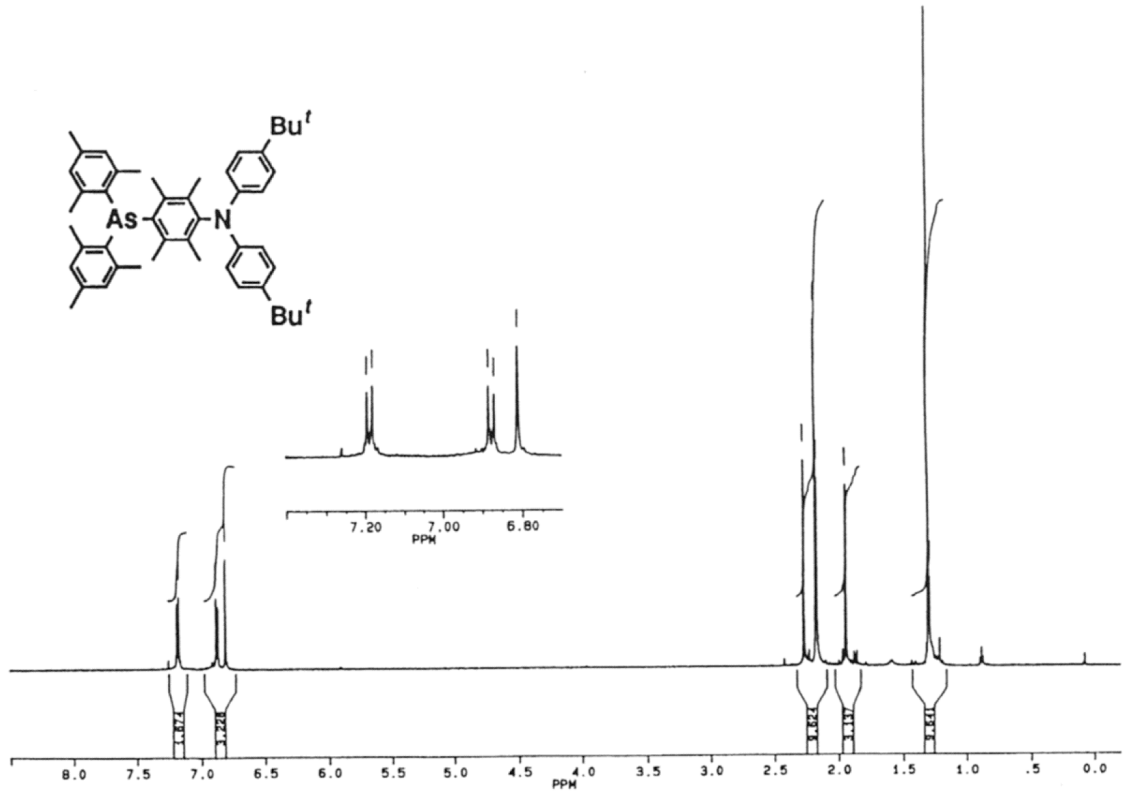

Figure 15. ^{1}H NMR (600 MHz, $CDCl_3$) spectrum of **4aA**.

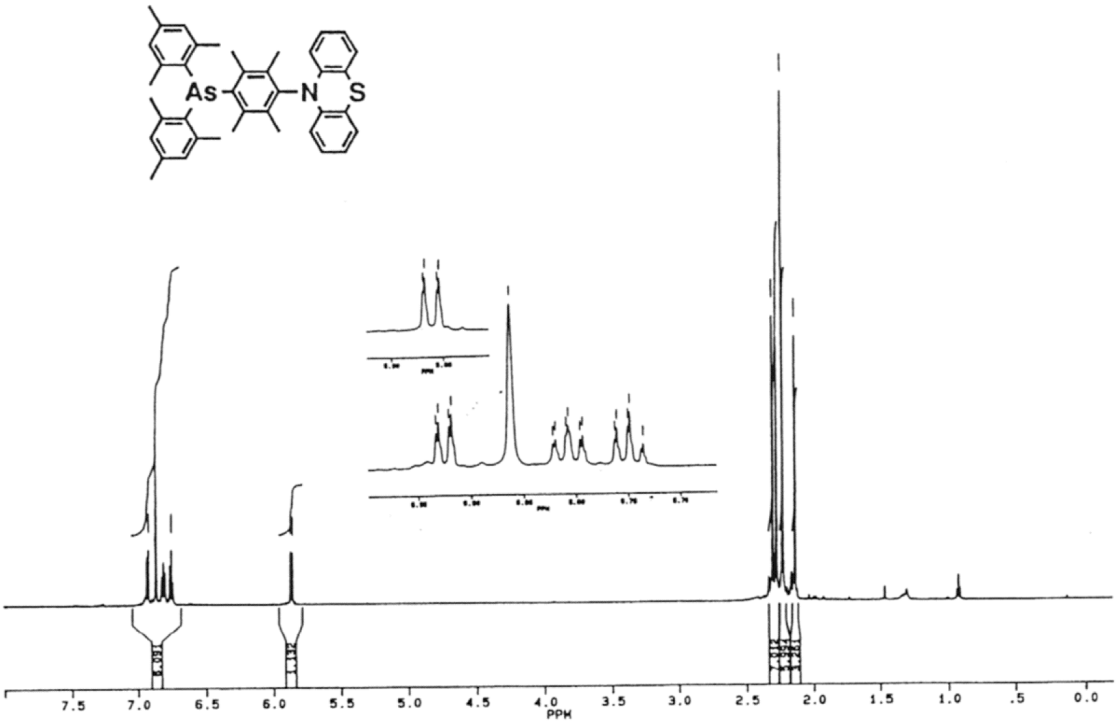

Figure 16. ^{1}H NMR (600 MHz, $CDCl_3$) spectrum of **4bA**.

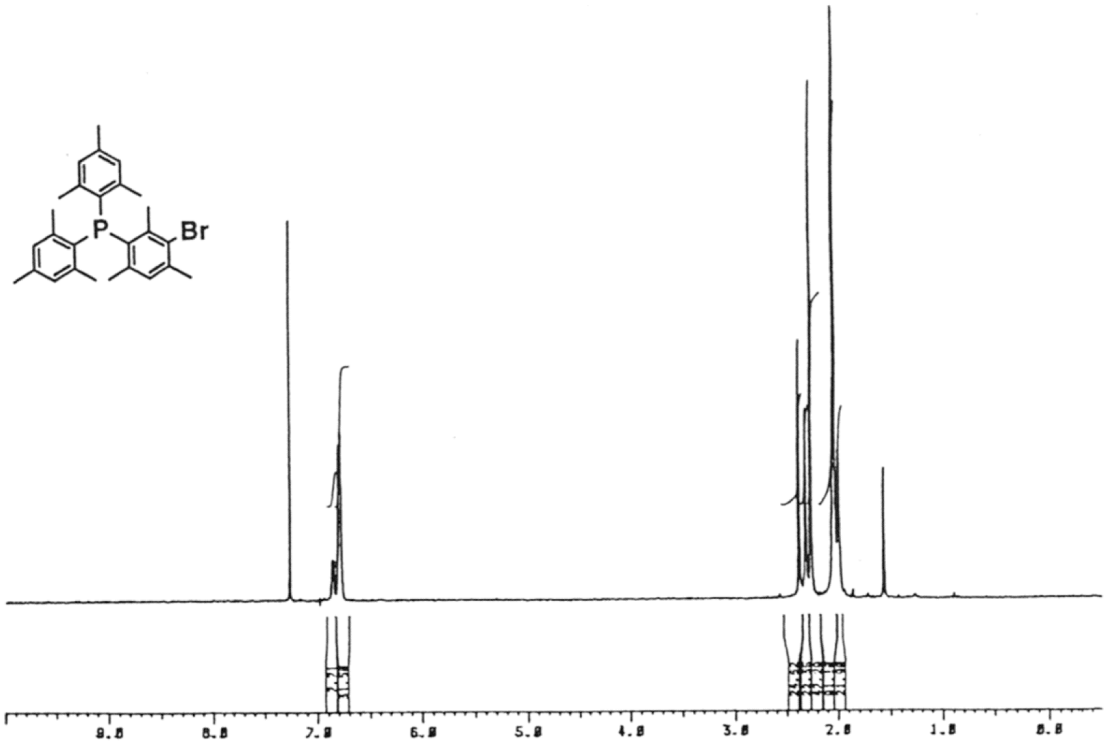

Figure 17. ^{1}H NMR (200 MHz, $CDCl_3$) spectrum of **5aP**.

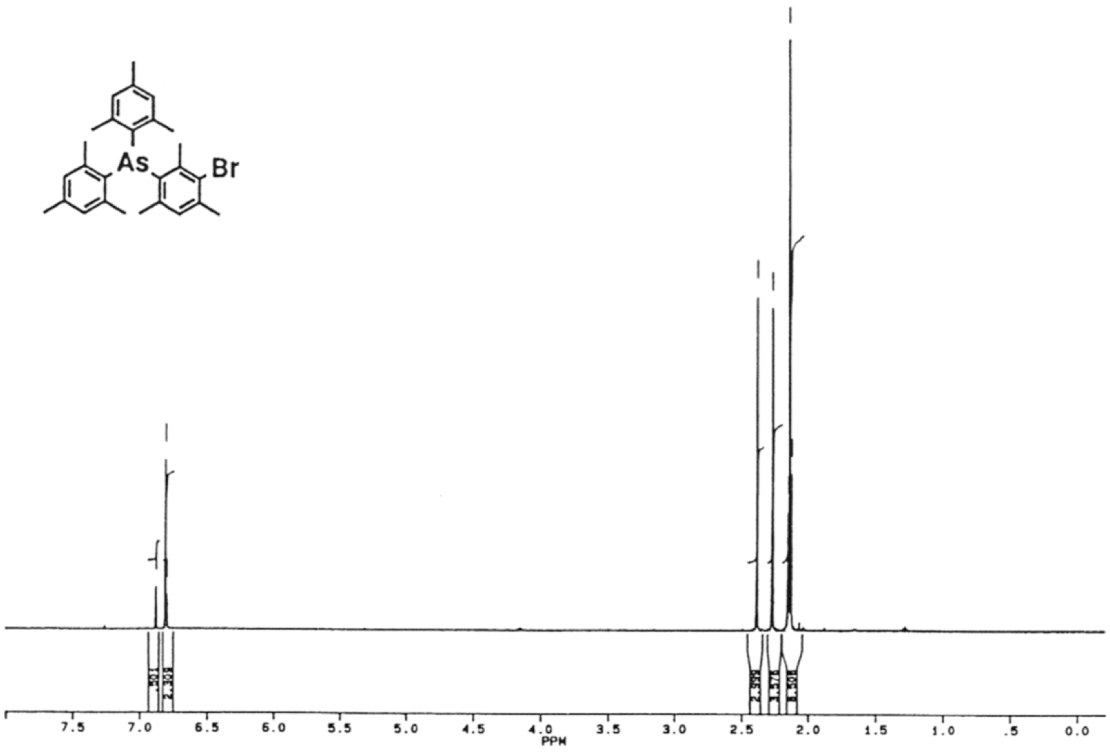

Figure 18. ^{1}H NMR (600 MHz, $CDCl_3$) spectrum of **5aA**.

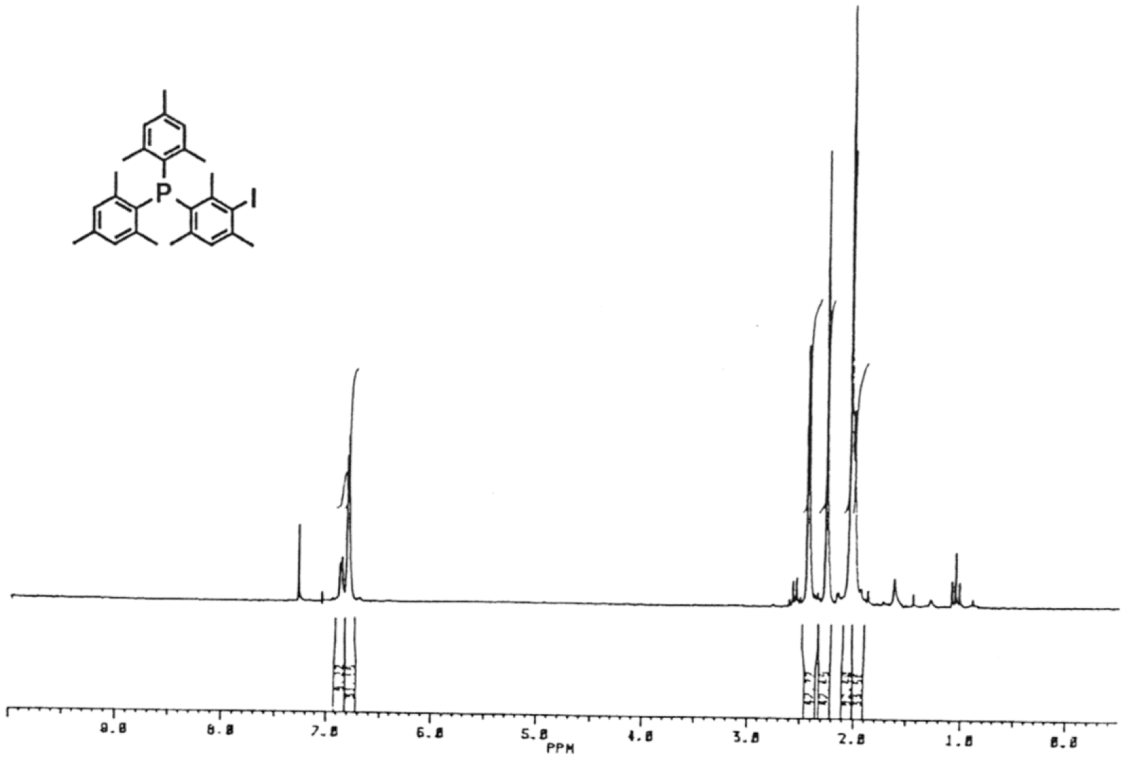

Figure 19. ^{1}H NMR (200 MHz, $CDCl_3$) spectrum of **5bP**.

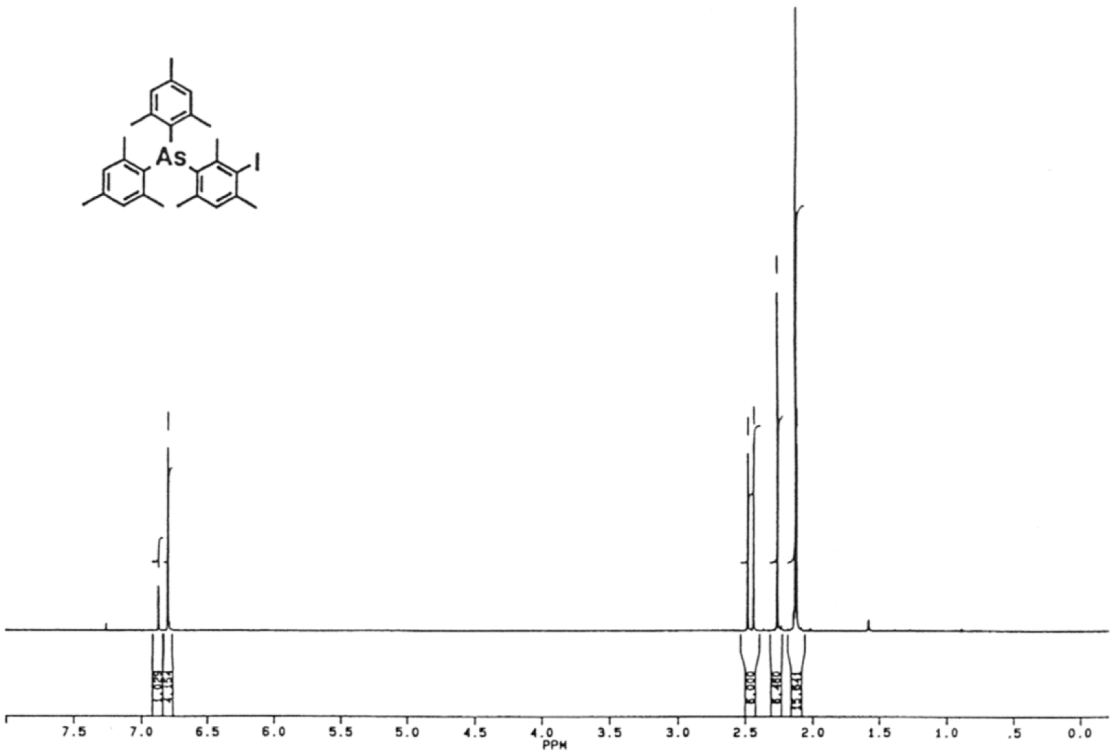

Fgure 20. ^{1}H NMR (600 MHz, $CDCl_3$) spectrum of **5bA**.

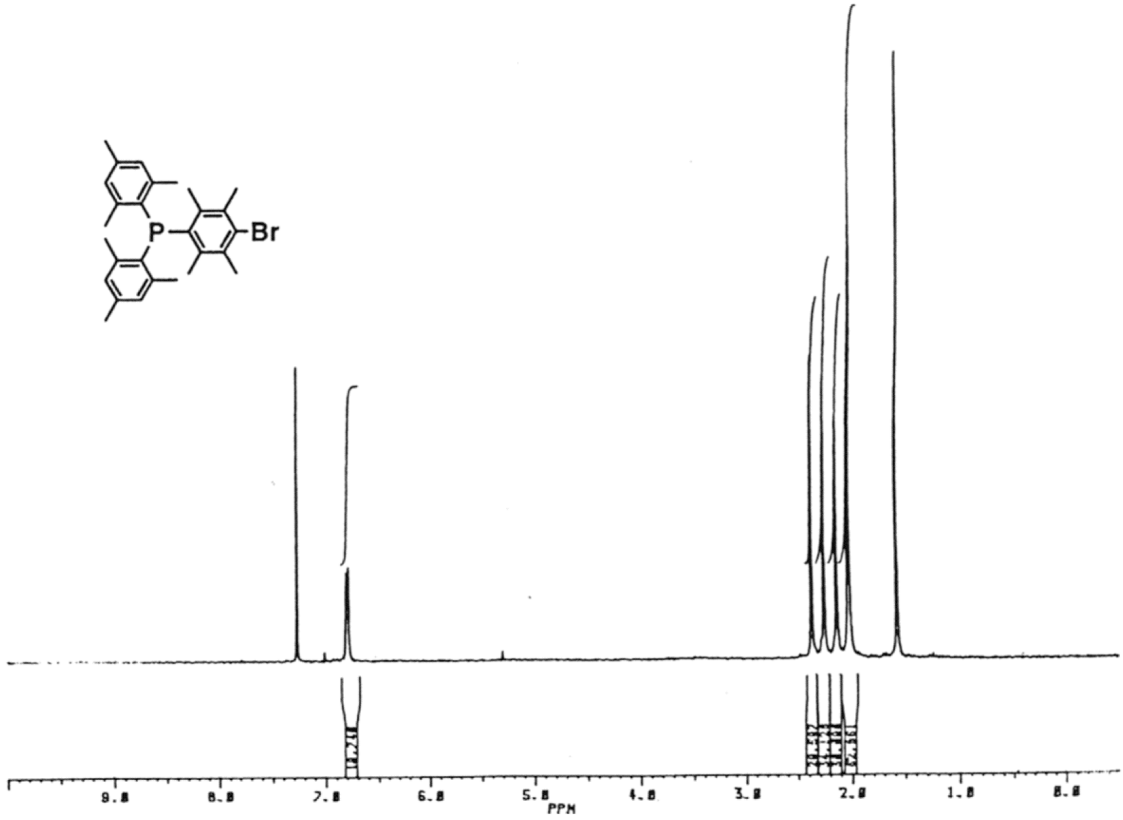

Fgure 21. ^{1}H NMR (200 MHz, $CDCl_3$) spectrum of **6aP**.

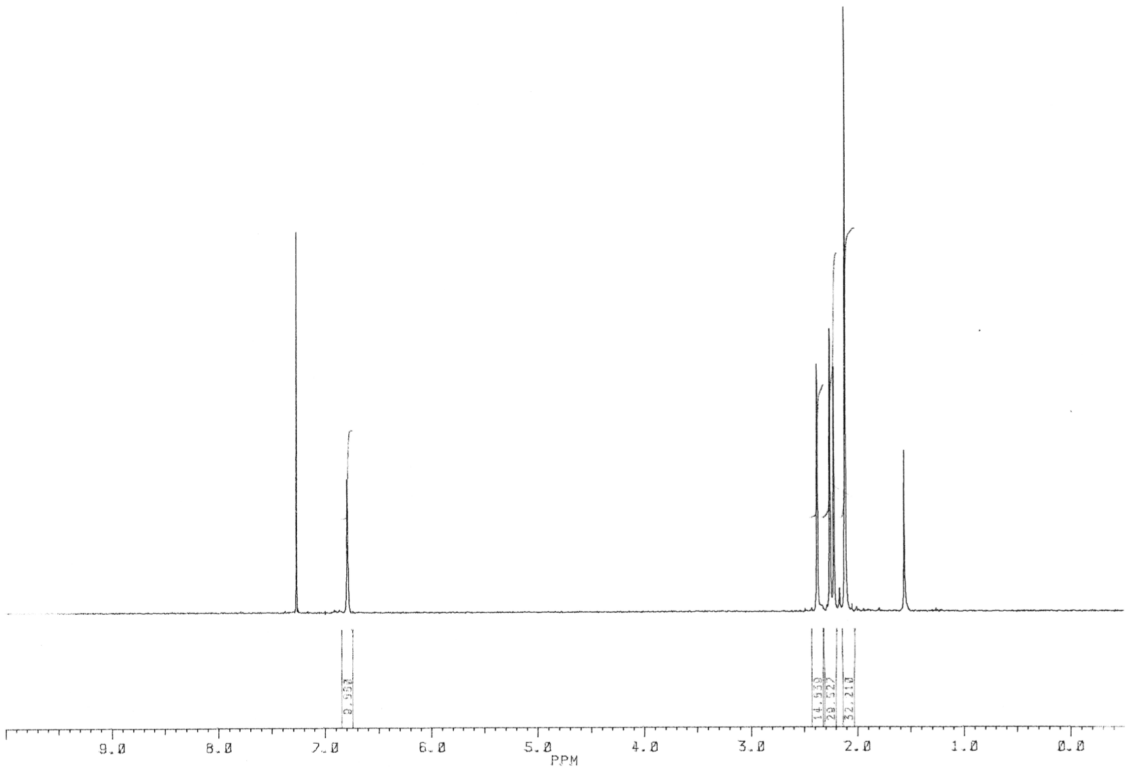

Fgure 22. ^{1}H NMR (200 MHz, $CDCl_3$) spectrum of **6aA**.

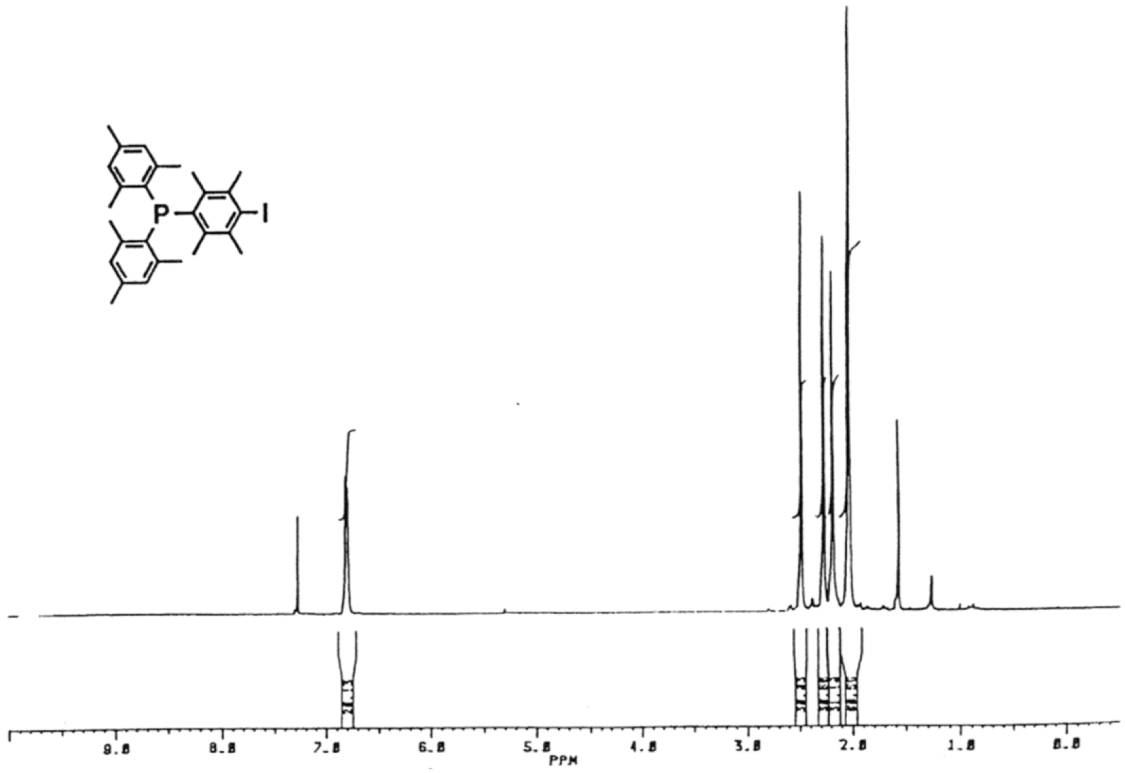

Fgure 23. ^{1}H NMR (200 MHz, $CDCl_3$) spectrum of **6bP**.

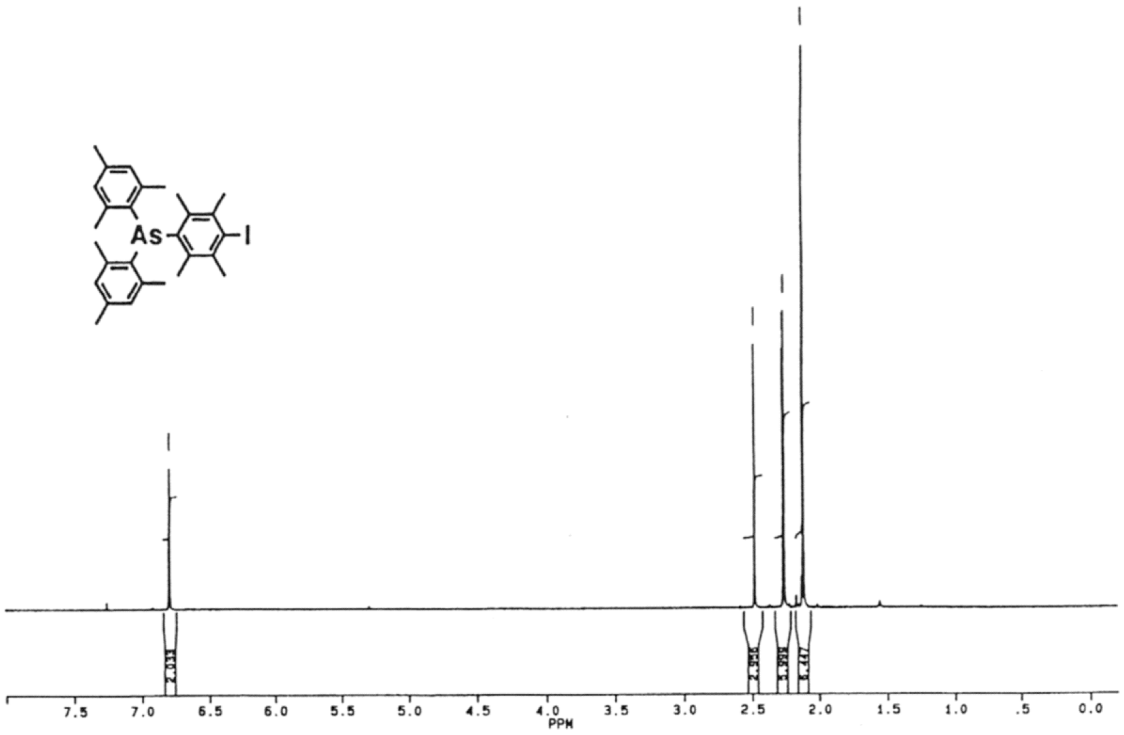

Fgure 24. ^{1}H NMR (600 MHz, $CDCl_3$) spectrum of **6bA**.

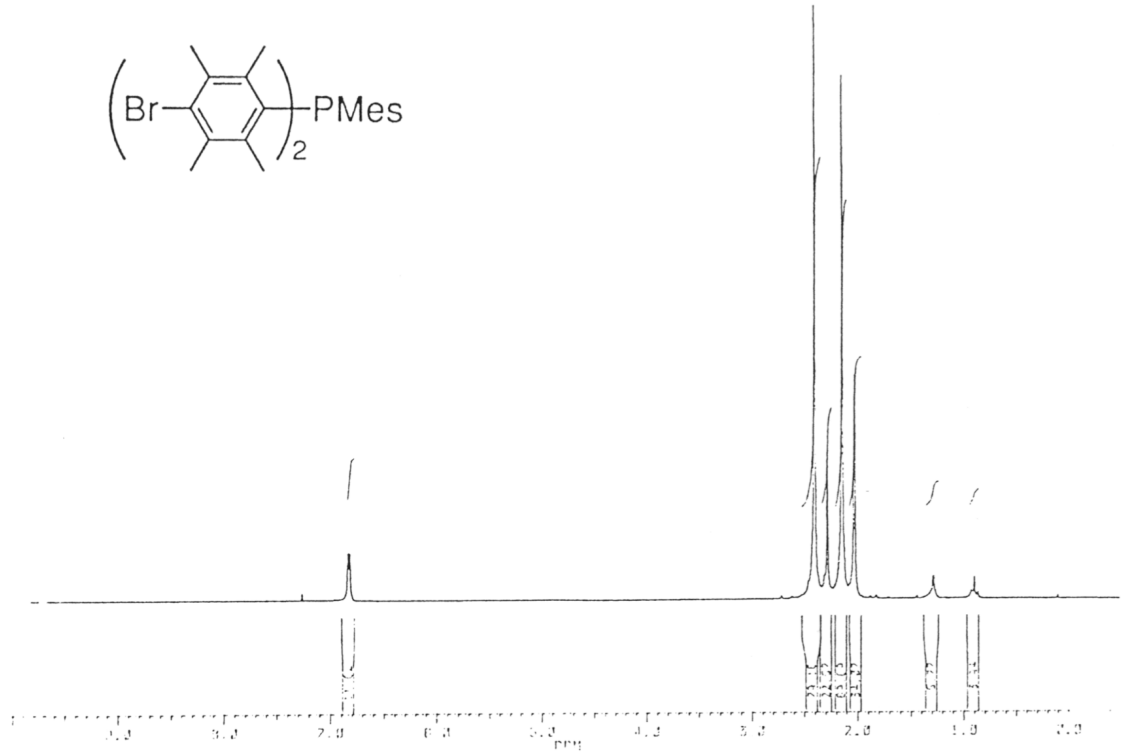

Fgure 25. ^{1}H NMR (200 MHz, $CDCl_3$) spectrum of **7**.

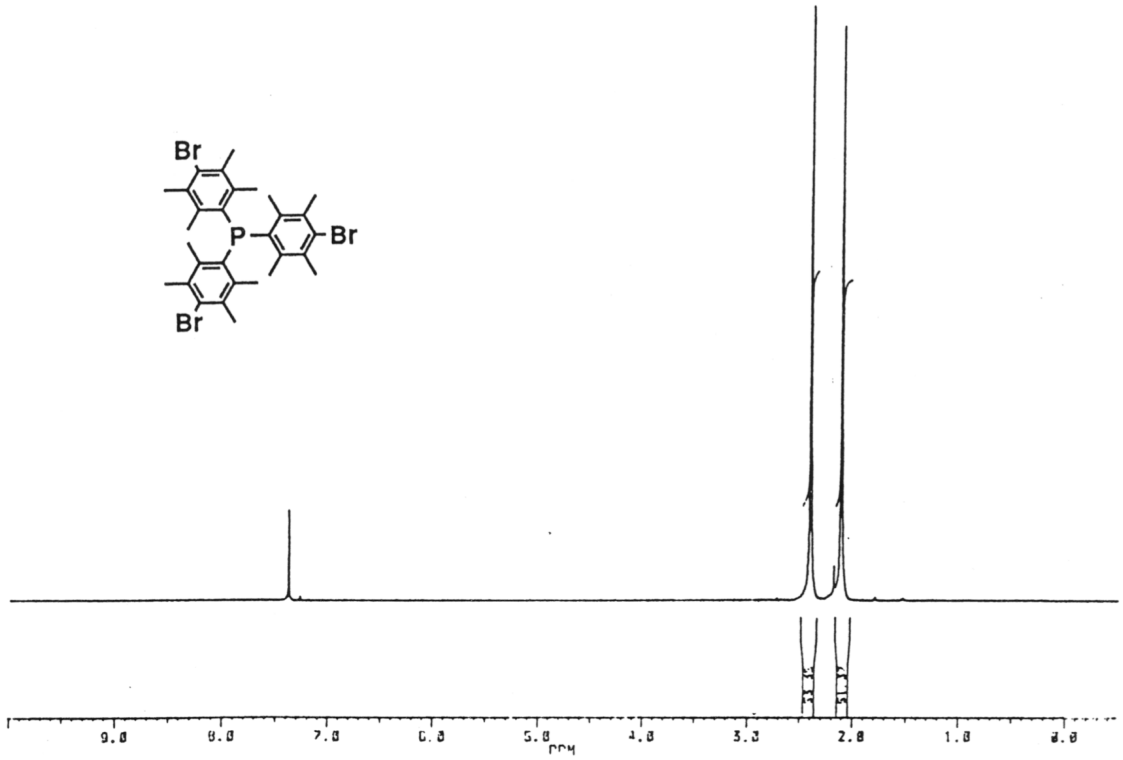

Fgure 26. ^{1}H NMR (200 MHz, $CDCl_3$) spectrum of **8**.

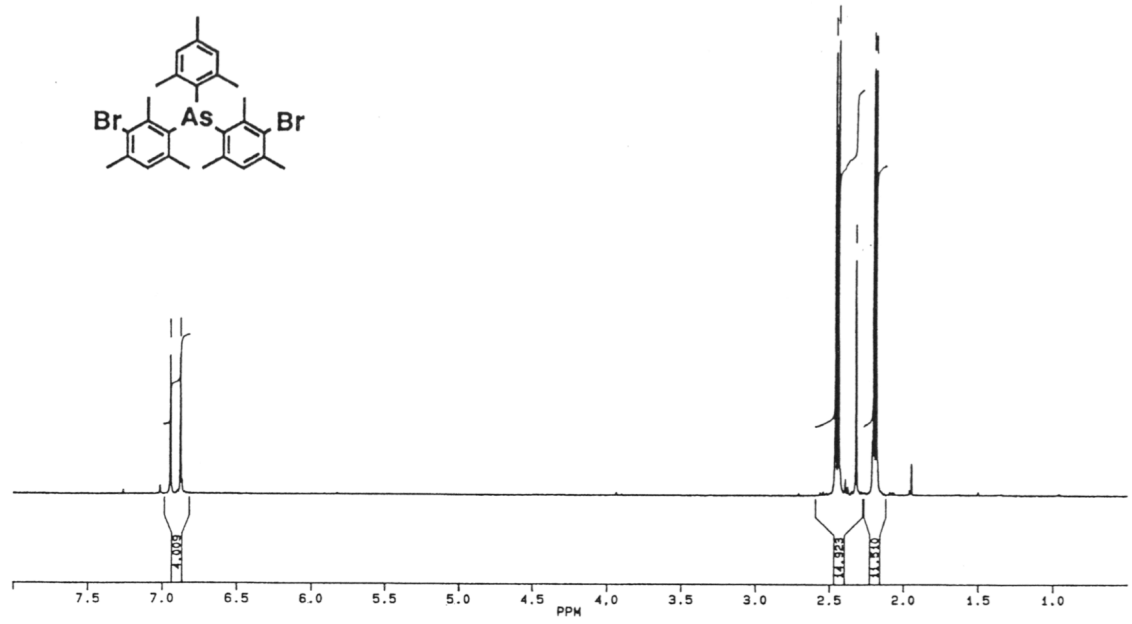

Fgure 27. ^{1}H NMR (600 MHz, $CDCl_3$) spectrum of **9**.

References

(1) Smith, L. I.; Moyle, C. L. *J. Am. Chem. Soc*. **1933**, *55*, 1676.